ISBN: 978-3-95450-207-3 doi:10.18429/JACoW-MEDSI2018-WEOAMA04

THE DESIGN OF EXACTLY-CONSTRAINED X-RAY MIRROR SYSTEMS FOR SIRIUS

R. R. Geraldes, G.V. Claudiano, L.M. Volpe, M. S. Souza, A. Sikorski, V. Z. Ferreira, L. Sanfelici, H.C.N. Tolentino, H. Westfahl Jr., Brazilian Synchrotron Light Laboratory (LNLS), Brazilian Center for Research in Energy and Materials (CNPEM), 13083-970, Campinas, Sao Paulo, Brazil.

Abstract

The first set of Sirius beamlines is expected to start operating in early 2019. Regarding X-ray mirror systems, a single design concept has been possible thanks to the standardization of side-bounce fixed-shape mirrors. To preserve the extreme quality of both the mirror figures and the source, the main design targets were minimizing mechanical and thermal distortions in the mirrors while maximizing mechanical and thermal stabilities. A deterministic high-resolution exactly-constrained flexure-based mirror support provides pitch tuning within 100 nrad and resonances above 150 Hz, while dealing with clamping and thermal expansion effects. The adopted cooling strategy was indirect cryocooling via cryostats, drastically minimizing thermal gradients and distortions in the mirrors, decoupling vibration sources and simplifying cooling circuits. Finally, a 5-degree-of-freedom granite bench, based on high-resolution levellers and air-bearing solutions, support the vacuum chamber, on which the internal mechanics is stiffly mounted. The specifications, design and partial results are presented.

INTRODUCTION

The design of mirror systems is one of the most revisited topics in beamline designs, since ever-increasing power management and figure error requirements continuously drive either innovative or optimized concepts, particularly for cooling and figure shaping [1–6]. For many solutions, however, it is often unclear how complex mechanics and cooling schemes may limit performance either in terms of slope errors or mechanical stability.

To comply with height and slope budget errors as low as a few nanometers and tens of nanoradians, respectively, Sirius X-ray mirrors were standardized in fixed-figure configuration, thus preventing the use of benders. Next, looking forward to superior passive mechanical stability, the decision for side-bounce deflection standardization was made. These two conditions, together with generally low absorbed power levels, i.e. below 50 W, have created the opportunity for the development of an alternative standard design for mirror systems, as illustrated in Fig. 1.

From the experience gained with the High-Dynamic Double Crystal Monochromator (HD-DCM) [7], deterministic design concepts have been applied to seek simple yet accurate and highly-stable thermo-mechanical solutions. Details about the vacuum vessel, cryocooling scheme based on cryostats and cooling braids, fixation of the mirrors and internal mechanics are given in the following sections. More information about the granite bench and the designing process for the mirrors are found in [8] and [9], respectively.

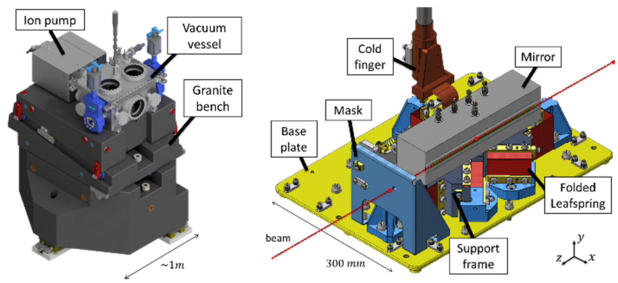

(a) (b)

Figure 1: Example of the new standard mirror systems for Sirius X-ray beamlines. (a) Vacuum vessel on granite bench; (b) mirror mounted to fine-tuning mechanism.

CONCEPTUAL DESIGN

The concept of the mirror systems was, from the very beginning, based on a few deterministic design guidelines. From the bottom to the top, the mirrors should be built on highly stable granite benchs, having only as many of degrees of freedom (DoF) as those necessary for positioning and alignment at the beamline [8]. Then, as approached in the HD-DCM, the vessel should be treated as an interface between the mirror and the bench, and by no means as a reliable and stable mounting structure in itself. Next, the mirrors should be deterministically fixed to an UHV-compatible high-resonance-frequency fine-tuning mechanism, which should be directly mounted to the vessel to benefit from the high stiffness of the bench. Finally, mechanically complex colling schemes should be avoided. Then, gathering the specifications, error budgets and alignment requirements for the mirrors of the first set of Sirius X-ray beamlines, common ground could be defined for the development of standard systems. The summarized specs are gathered in Table 1.

Table 1: X-ray Mirror Systems Summarized Specs

Description	Spec
Ry range:	> 1 mrad
Ry resolution:	< 100 nrad
Ry stability:	< 30 nrad $RMS_{2.5kHz}$
Resonances:	> 150 Hz
Thermo-mechanically induced slope errors:	< 50 nrad
Power load:	< 50 W
Cooling scheme:	indirect cryocooling via copper braid and cryostat

Mechanical Eng. Design of Synchrotron Radiation Equipment and Instrumentation MEDSI2018, Paris, France JACoW Publishing
ISBN: 978-3-95450-207-3 doi:10.18429/JACoW-MEDSI2018-WEOAMA04

Vacuum Vessel

The vacuum vessel module is depicted in Fig. 2. The stainless-steel vessel consists of a main square-shaped box and a top flange, sealed by means of aluminium wire. In the main vessel, all the required electrical feedthroughs for the motors, encoders, temperature sensors and heaters used in the internal mechanism are available, so that the mirror can be functionally tested before the lid is put on. It also has ports for: the entrance and exit of the beam (both with gate valves); viewports, which are also used for accessibility during assembly and maintenance; the standardized 600 L ion pump; vacuum sensors; and venting valves. The top flange hosts the cryostat port and auxiliary viewports.

A few key design choices regarding the chamber were made to improve the overall mechanical stability of the assembly. Firstly, benefiting from some torsional compliance of an open box, four contact pads are machined at the outer limits of the bottom surface of the vessel to deterministically define the mounting points on the granite. Thus, fixation lever-arms and, consequently, the rotational vibration modes of the chamber can be maximized. The preload is made through four bolts in extended ears in the bottom flange. Then, to optimize the stiffness chain between the internal mechanism and the granite by preventing excessive bending of the vessel's bottom flange due to the vacuum forces (and a possible loss of contact with the granite), a central pad is also machined in the center of the bottom surface and is preloaded against the granite by means of a SMW workpiece positioning system. Finally, the suspension frequency of the ion pump is also optimized by a stiff pre-loaded connection to the granite.

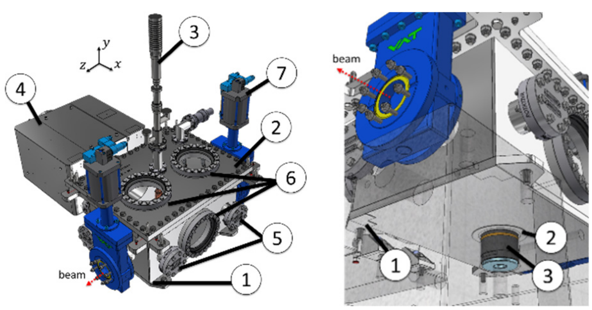

a) b)

Figure 2: (a) Isometric view of vessel module: (1) main vessel, (2) top flange, (3) cryostat, (4) ion pump, (5) electrical feedthroughs, (6) viewports and (7) gate valves. (b) Isometric view through transparent granite, highlighting the outer (1) (x4) and central (2) contact pads, and the workpiece positioning system embedded in the granite (3).

These choices make in-situ baking a potential problem, due to temperature limits and thermal expansion effects between the vessel and the granite. In addition to that, designing the internal mechanism to allow for both low and high temperature ranges would offer additional limitations in terms of stresses. Finally, decoupling the vessel from the granite for baking might lead to alignment issues. All considered, in-situ baking was considered a disadvantageous option. Therefore, to complement pre-assembly baking of the parts, a hot-nitrogen purging system is currently under development for in-situ pumping improvement.

Mirror Fixation

To achieve high-stability performances without active dynamic stabilization, two basic approaches are mitigating disturbance sources and designing for high-frequency resonances. For the mirrors: the first is obtained by decoupling the cooling source via braids; whereas the latter depends on materials and design. Practical limitations are given by the compromise between high clamping forces for high contact stiffness and the introduced stresses and deformations, which might spoil mirror figures.

For the HD-DCM, a three-point flexure-based solution for fixing the crystals with deterministic mechanical and thermal performance was implemented [10]. There, dynamic coupling above 1kHz was achieved, while dealing with thermal expansion effects between the crystals and their supports for temperature differences as high as 100 K. Hence, a similar solution was considered for the mirrors, as shown in Fig. 3.

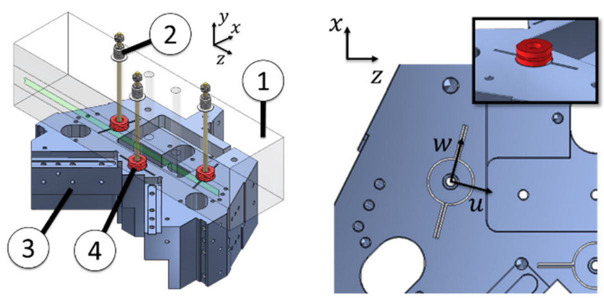

a) b)

Figure 3: Mirror fixation concept with flexures and flexural-hinges: a) isometric view of the assembly: (1) mirror (transparent for visualization), (2) threaded rods, (3) support frame and (4) hinges; b) top view of one of the flexures, indicating its local coordinate system (*uwy)*, and inset with hinge.

Regarding thermal effects, the three flexures machined in a support frame create a thermal center with respect to which the optics may deterministically shrink or expand. Although this concept alone was enough for the crystals in the HD-DCM, the extreme error budget requirements of the mirrors led to the development of an additional elastic layer. Indeed, since each flexure has one weak translation (u) and one weak rotation (R_w), but high stiffness in all other directions, machining height and flatness limitations in the contact surfaces of the support and the mirror would lead to bending moments and, consequently, unacceptable deformations in the mirrors. This problem was reduced by adding flexural hinges between the mirror and the flexures, having the compliant rotation of the hinge (R_u) perpendicularly aligned to the compliant rotation of the flexure. Thus, a spherical joint is emulated in each contact region and a *quasi*-kinematic mount is achieved.

Naturally, if compared to the crystals in the HD-DCM, lower modes can be expected, due to the much larger masses of the mirrors and limitation in clamping forces. Nonetheless, modes above 200 Hz are typically feasible, provided that the fixation points in the mirror are properly

ISBN: 978-3-95450-207-3 doi:10.18429/JACoW-MEDSI2018-WEOAMA04

chosen. As for preload and the connection to the cooling braids, controlled nearly-constant forces can be applied via threaded rods and proper arrangements of spring-washers.

Internal Mechanics

Considering that all the necessary DoF of the mirrors should be covered by the granite bench, the internal mechanics may simply provide a few high-resolution DoF with enough range to complement that of the bench when necessary. Thus, after the development of the HD-DCM, the possibility of designing short-range mechanisms for mirrors based on folded leafsprings (FLS) was very appealing due to several reasons.

Firstly, clean, high-resolution, high-repeatability and nearly frictionless mechanisms are possible. Secondly, as FLS constrain a single DoF [11], not only is it relatively simple to add or remove DoF, but also the support frame of the mirror may be exactly-constrained, preventing bending moments and deformations from connections with other parts, which would be, otherwise, propagated to the mirror to some extent. In addition to that, a thermal center can be designed for the support, so that its working temperature may have much more design flexibility while thermal expansions are conveniently handled. In that sense, another advantage is that FLS may also work as an efficient thermal isolation layer between parts at different temperatures. Moreover, they do not present shortening effects, as many flexural options do, so that parasitic effects can be reduced.

Another key advantage in this concept is that through careful design the mechanism stiffness in different axes can be optimized so that the driving forces can be significantly reduced. This not only expands the range of actuation options, allowing for simple and cost-effective piezowalkers, for instance, to be selected, but also paves the way for dynamic mirror systems, if active mirrors are to be developed for improved stability or scanning performance. In fact, a scanning Kirkpatrick Baez (KB) system is already envisioned for Sirius CARNAUBA beamline. So, within this conception the resolution is simply defined by the actuator resolution and/or the actuation lever-arm; the range, by the driving force capacity, or ultimately by the stresses in the FLS; whereas linearity, repeatability and parasitic motion are direct outputs of the concept and its realization.

Figure 4 shows the proposed internal mechanism for the first mirror of CATERETE beamline: CAT-1-VFM. The fine pitch (*Ry*) DoF is implemented by means of: three vertically-oriented FLS, constraining the vertical translation *Ty*, and the two rotations R_X and R_Z; and two horizontally-oriented FLS, constraining the two horizontal translations *Tx* and *Tz*, and defining the rotation axis and the thermal centre of the mechanism. The actuation is made with a linear piezo-walker actuator preloaded by a spring. The selection of this low-cost actuator was driven by resolution, force, range, control options, volume, UHV compatibility and cost. Comparing piezo-walker and piezo-stack actuators, for example, the first have significant range and volume advantages, at the same time that they may also result in improved passive stability. Indeed, piezo-stacks are active systems which may suffer from control noise and thermal drift. With a lever-arm of about 80 mm, step sizes of 100 nrad should be feasible. Moreover, the optimized FLS design allows for 3 mrad stroke with less than 5 N, leaving at least 15 N for preloading forces without exceeding the capacity of the actuator, so that good contact stiffness between the actuator tip and the support can be achieved.

For metrology and feedback, resolution in the order of 10 nrad RMS up to 2.5 kHz was desired to allow for online local in-position stability measurements. Absolute linear encoders with 1 nm resolution were selected over other non-contact probes options, such as capacitive sensors and interferometers (IFM). The reasons were: resolution and range are not conflicting factors, as they are in capacitive sensors; alignment tolerances are broader than in most IFM options; as in capacitive probes, but differently from IFM, absolute encoders save time in homing and alignment procedures; electronics are simpler and free of multiple-channel constraints; costs can be a factor 3 or 4 smaller.

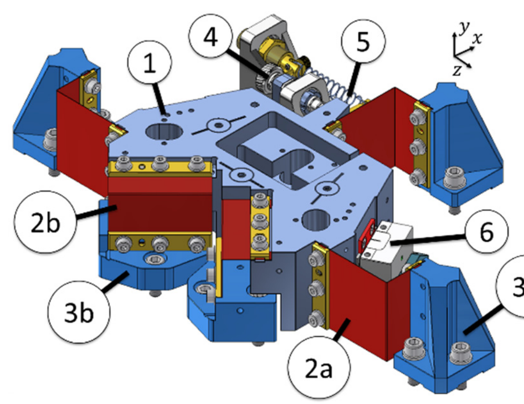

Figure 4: CAT-1-VFM mechanism isometric view: (1) support frame; (2) vertical (a) (x3) and horizontal (b) (x2) FLS; (3) vertical (a) (x3) and horizontal (b) (x2) FLS supports; (4) piezo actuator; (5) preload spring; and (6) optical encoder (x2).

Cooling and Thermal Management

Silicon, which is the substrate material of all X-ray mirrors of the first set of Sirius beamlines, is known for remarkable thermal properties at low temperatures. Indeed, not only does the thermal expansion cross zero around 125 K, but also the thermal conductivity even exceeds that of copper for temperatures between 80 and 150 K. Thus, when compared to room-temperature operation, and particularly if the absorbed power levels and power densities are low enough, having the operational temperature of a mirror around 125 K may considerably reduce its thermal gradients (due to the high thermal conductivity) and nearly eliminate thermal bumps in the footprint (due to the very low thermal expansion). Considering the very small numbers in height and slope error budgets, this becomes an interesting option if the remaining challenges of working in cryogenic temperatures can be properly handled.

Regarding design, different alternatives can be envisioned once the heat conduction in the silicon body itself may not be the bottleneck in the heat extraction chain. For low powers, an elegant solution consists in indirectly cooling the mirror via a copper braid and a cryostat, as adopted

ISBN: 978-3-95450-207-3 doi:10.18429/JACoW-MEDSI2018-WEOAMA04

for handling 20 W in an artificial channel-cut monochromator at the XFEL [12]. Some key advantages of this solution over conventional water cooling schemes are: the drastic reduction in number of parts and masses around the optics; the decoupling from the cooling vibration source; and the elimination of water-vacuum interfaces or vacuum guards. Therefore, this was chosen as the standard solution for Sirius X-ray mirrors. In most cases, with power levels below 10 W, the solution is fairly straightforward. A few cases, however, do require some more work as they approach 40 or 50 W, which seems to be a practical limit due to the limited conductivity of the interfaces and the braids.

In cryogenic applications materials selection deserves special attention. When dealing with flexures linking parts with large temperature differences, two opposite choices can be considered. Either high-conductivity materials may be used to prevent excessive temperature gradients, or low-conductivity materials with small thermal expansion coefficients and high yield strengths are required, so that the large gradients may result in bearable deformations and stresses. For the support frame, aluminium was the material of choice because of: availability and costs; low density, reducing mass and inertia for improved dynamic performance of the assembly; good thermal diffusivity, allowing for faster thermal stabilization and temperature control; and small bending sensitivity, reducing bending moments and deformations. Thus, differently from the HD-DCM in which the invar flexures worked as an efficient thermal resistance, the mirror support flexures resulted in poor thermal insulation. Nonetheless, the insulation requirements between mirror and frame could be easily fulfilled by the hinges, made of Ti-6Al-4V. Moreover, considering 125 K as the target temperature of the mirrors, 283 K becomes a suitable operational temperature for the support frame, since the secant thermal expansions of aluminium and silicon match, minimizing in-plane elastic forces introduced by the deflection of the flexures.

Finally, with such large cold parts, if thermal shields were not used, blackbody radiation would generally be the major player in heat transfer to the optics, easily overcoming the beam load. Therefore, shields at about 240 K, also cooled by the cryostat via copper braids, almost completely cover the internal mechanics.

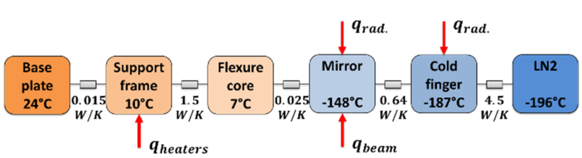

Figure 5: Simplified lumped-mass model for CAT-1-VFM, with expected temperatures and thermal conductivities.

Figure 5 and Figure 6 respectively show the simplified lumped-mass thermal model for CAT-1-VFM, with temperatures and thermal conductivities, and thermal FEA for the mirror, the hinges and the support frame in full operational conditions. It can be seen that the temperature in the body of the aluminium support frame is nearly constant and that the thermal gradient in the mirror is expected to be in the order of 0.1 K for a beam load of 9 W. In the hinge, on the other hand, a temperature drop of 150 K is seen. Thus, once the stresses in the flexures of the support frame are negligible, in the hinges it may exceed 100 MPa.

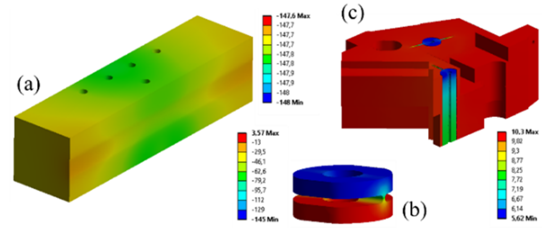

Figure 6: Thermal FEA (in °C) for the key parts in CAT-1-VFM mirror system under full operational loads (9 W beam + radiation), shown separately for readability: (a) mirror, (b) Ti-6Al-4V hinge; (c) aluminium support frame.

RESULTS

As a proof of concept, a prototype based on CAT-1-VFM mechanical system was built and characterized in air on an optical table (see Fig.7). Beginning with the results of modal analysis, Table 2 lists its first eigenmodes, showing remarkable agreement between FEA simulations and experimental data, which not only validates the concept with respect to the high-frequency targets, but also proves that the designing process has been consistent.

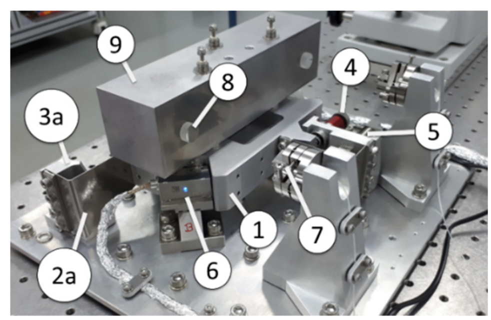

Figure 7: CAT-1-VFM prototype: (1) support frame; (2a) vertical FLS (2); (3a) vertical FLS support; (4) piezo actuator; (5) preload spring; (6) optical encoder; (7) IFM; (8) IFM target mirror; (9) dummy mirror.

Table 2: Modal Analysis for CAT-1-VFM Prototype

Mode	FEA [Hz]	Experimental [Hz]
1 (T_x)	249,7	250
2 (R_y)	312,5	313
3 (T_z)	342,4	341
4 (T_y)	408,9	403
5 (R_z)	602,5	554
6 (R_x)	614,9	851

Next, the motion performance was evaluated for resolution, range, linearity, parasitic motion errors and position stability. Figure 8 shows an open-loop resolution measurement with a 22nm-resolution actuator and the average signal of two 5nm-resolution optical encoders. With lever-arms of 0.1 and 0.08 m, respectively, it is clear that the step size is limited by the actuator and that the feedback signal has significant noise limitations. For the final systems, better resolution is expected in both actuation and metrology.

ISBN: 978-3-95450-207-3 doi:10.18429/JACoW-MEDSI2018-WEOAMA04

Moreover, the asymmetry is step-size is a known behaviour in this type of piezo linear actuator.

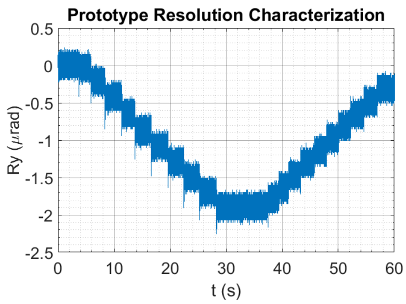

Figure 8: CAT-1-VFM prototype open-loop resolution characterization with preliminary piezo actuator and optical encoders.

With sufficient alignment tolerances in the encoders, a total range of ± 5 mrad was achieved. Then, an Elcomat 3000 autocollimator was used to measure the linearity and *Rx* and *Rz* parasitic rotations an as a function of the feedback signal. Figure 9 shows that the residual errors from a linear fit (ϵ_{Ry}), as well as the parasitic rotations are below ± 0.1% of the motion range, and mostly within ± 2 µrad. Additionally, as the two encoders are orthogonal to each other, the parasitic translation in the *x* direction can be extracted from the two signals. Over the full range a symmetric parabolic runout of 2 µm was found.

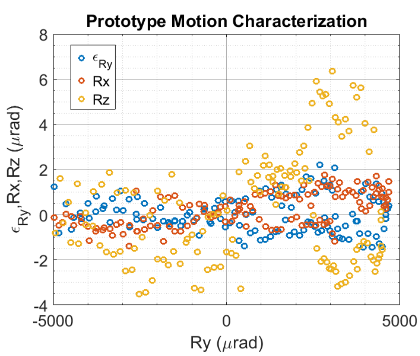

Figure 9: CAT-1-VFM prototype residual linearity errors (ϵ_{Ry}) and parasitic *Rx* and *Rz* rotations, as a function of the feedback signal.

The prototype still allowed for the evaluation of Lion Precision's C8-2.0 capacitive probes, tested in high and low-resolution modes, and SmarAct's PicoScale standard IFM as feedback sensors. Thus, all three alternatives could be compared, as summarized in Table 3. In terms or range, as expected, the encoders have a significant advantage. Regarding linearity, all sensors showed similar performance. As for stability, looking at the power spectrum density plots, all sensors seemed to be noise-limited over most of the large frequency range. In the table, the cumulative amplitude spectrum up to 2.5 kHz is given and the best results were achieved with the capacitive probe in high-resolution mode. Similar levels are expected from the 1nm-resolution encoders. Finally, the IFM was tested as an option of direct metrology (see Fig. 7), as the other sensors work over the support frame. Thanks to the high-frequency modes of the system and the limited bandwidth of the disturbance sources, no significant differences were observed. As similar conditions are expected in real operation, having the encoders as feedback should be sufficiently reliable.

Table 3: Sensors Comparison at CAT-1-VFM Prototype

Mode	**Range**	ϵ_{Ry}	**Stability (RMS)**	
	[mrad]	[µm]	***Ry*** [nrad]	***x*** [nm]
Encoder	± 5	< 3	55	5
Cap. (h.r.)	±0,25	–	10	1
Cap. (l.r)	±1,25	< 2	50	3
IFM	± 2,95	< 1	35	3

Lastly, some results reporting problems in mirror coatings at low temperatures, especially involving multilayers, can be found [13]. Thus, to validate the use of cryogenic temperatures, the CARNAUBA beamline CAR-1-MC mirror, with Rh and Ni coating layers, has been cycled between 125 K and room temperature a few times. Transversal height measurements performed with a Fizeau DynaFiz interferometer before and after cycling are shown in Fig. 10, from where no risks or problems could be identified. Complementary measurements with results for the deformations caused by the clamping forces can be found in [8].

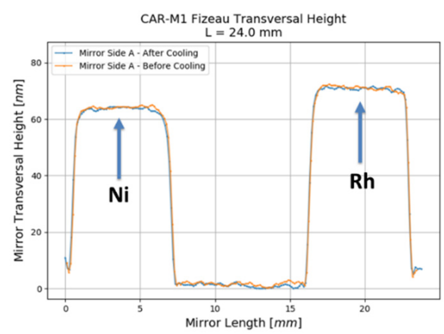

Figure 10: Transversal height measurement with Fizeau DynaFiz for CARNAUBA CAR-1-MC mirror, before and after cryocooling cycles. (Courtesy of OPT group.)

CONCLUSION

By means of deterministic design and system approach, an innovative concept for mirror systems has been developed, in which thermal, mechanical and optical challenges are simultaneously addressed. Decoupling vibrations sources via copper braids, preventing stresses by means of FLS, flexures, hinges and proper material selection, and limiting DoF and ranges of motion were some of the key aspects that resulted in this cost-effective high-performance system. Successful results in terms of eigenfrequencies and motion have been demonstrated in a functional prototype in air, while thermal and clamping performances started to be investigated in parallel. In the forthcoming months, a full set of complete mirrors systems shall be commissioned.

ACKNOWLEDGEMENTS

The authors would like to gratefully acknowledge the funding by the Brazilian Ministry of Science, Technology, Innovation and Communication and the contribution of the LNLS team.

ISBN: 978-3-95450-207-3 doi:10.18429/JACoW-MEDSI2018-WEOAMA04

REFERENCES

[1] R. Baker *et al.* "New generation mirror systems for the ESRF upgrade beamlines", J. Phys.: Conf. Ser. 425 052015, 2103.

[2] M. Mattenet *et al.*, "Optimization of X-ray mirror mounting: test bench and results", *Proc. MEDSI 2012*, Shanghai, China, Oct. 2012.

[3] C. Colldelram *et al.*, "The nanobender: a new X-ray mirror bender with nanometer figure correction", in *Proc. MEDSI 2016*, Barcelona, Spain, Sep. 2016.

[4] L. Zhang *et al.*, "LCLS-II KB mirror systems: technical challenges and solutions", presented at MEDSI 2016, Barcelona, Spain, Sep. 2016.

[5] L. Zhang *et al.*, "Minimization of mechanical constraint effects of Eutetic GaIn as thermal interface", presented at MEDSI 2016, Barcelona, Spain, Sep. 2016.

[6] T. Noll *et al.*, "The generic mirror chamber for the European XFEL", in *Proc. MEDSI 2016*, Barcelona, Spain, Sep. 2016.

[7] R. Geraldes *et al.*, "The new high dynamics DCM for Sirius", in *Proc. MEDSI 2016*, Barcelona, Spain, Sep. 2016.

[8] R. Geraldes *et al.*, "Granite benches for Sirius X-ray optical systems", presented at MEDSI 2018, Paris, France, Jun. 2018, this conference.

[9] L. Volpe *et al.*, "Optimization method using thermal and mechanical simulations for Sirius high-stability mirrors", presented at MEDSI 2018, Paris, France, Jun. 2018, this conference.

[10] M. Saveri Silva *et al.*, "Thermal management and crystal clamping concepts for the new high dynamics DCM for Sirius", in *Proc. MEDSI 2016*, Barcelona, Spain, Sep. 2016.

[11] H. Soemers, "Flexural mechanisms", in *Principles for precision mechanisms*, Twente University, Twente, Netherlands. 2010.

[12] X. Dong *et al.*, "Design of a Cryo-Cooled Artificial Channel-Cut Crystal Monochromator for the European XFEL", in *Proc. SRI2015*, New York, USA, Jul. 2015.

[13] X. Cheng, "Thermal stress issues in thin film coatings of X-ray optics under high heat load", Université de Grenoble, Grenoble, France, 2014.